

## Experimental and Calculated Swelling Behavior of U-10 wt.% Mo Under Low Irradiation Temperatures

J. Rest and G. L. Hofman, Argonne National Laboratory, 9700 S. Cass Ave., Argonne, IL 60439, USA

I. I. Konovalov and A. A. Maslov, Bochvar Institute, Rogov St. 5, 123060 Moscow, Russia

### ABSTRACT

SEM photomicrographs of U-10 wt.% Mo irradiated at low temperature in the ATR to about 40 at.% burnup show the presence of cavities. We have used a rate-theory-based model to investigate the nucleation and growth of cavities during low-temperature irradiation of uranium-molybdenum alloys in the presence of irradiation-induced interstitial-loop formation and growth. In addition, the evolution of forest dislocations was calculated on the basis of dislocation loop growth and simultaneous climb and glide of unfaulted loops. Consolidation of the dislocation structure takes into account capture of interstitial dislocation loops and loss to grain boundaries. Cavities are nucleated when two gas atoms come together in the presence of at least one vacancy. Cavity growth occurs by the influx of gas atoms and/or vacancies. In turn, the free interstitial concentration, and thus (due to recombination) the free-vacancy concentration, depends on the dislocation density. Bias-driven growth of cavities can lead to substantial swelling of the alloy (void swelling). However, our calculations indicate that the swelling mechanism in the U-10 wt.% Mo alloy at low irradiation temperatures is fission-gas driven. The calculations also indicate that the observed bubbles must be associated with a subgrain structure. Calculated swelling and bubble-size-distribution are compared with irradiation data.

### INTRODUCTION

An important aspect of modeling the behavior of candidate LEU high-density uranium-alloy dispersion fuels is the identification of key irradiation-induced swelling mechanisms. The delineation of these physical processes facilitates the design of an optimal fuel type and provides confidence in irradiation performance in regions beyond those explored experimentally. Pure uranium and various alloys of uranium that exist in the orthorhombic  $a$ -phase (e.g., U-Zr-Nb) are poor performers under irradiation due to anisotropic growth that induces grain-boundary tearing and resultant breakaway swelling. U-10 wt.% Mo is one in a series of alloys designed to maintain uranium in a metastable

cubic phase. The “hope” for these stabilized alloys is stable swelling behavior throughout fuel lifetime.

Previous calculation [1] of the irradiation-induced swelling of U-10 wt.% Mo showed that the predicted swelling is a strong function of the steady-state value of the dislocation density. Increasing the dislocation density by a factor of 2 can mean the difference between gas-driven growth and bias-driven (void) growth. The bias-driven (void) growth mechanism results in significantly more swelling than the bubble-driven component and can lead to breakaway swelling behavior. Thus, it is important to identify the dislocation kinetics. In the past, both the U.S. and the Russian authors have partitioned the swelling calculations into various stages, e.g., dislocation nucleation and growth, void nucleation and growth, gas-bubble growth. However, this approach precludes the possibility that the bubble/void nucleation mechanism competes with the dislocation nucleation/growth mechanism for irradiation-produced defects (vacancies and interstitials). In addition, previous calculations of the dislocation density (taken as the interstitial loop line length) have resulted in an overprediction due to ignored constraints on the growth of the loop size distribution. The loops evolve until the spacing between loops reaches a distance characteristic of that separating crystalline defects such as dislocations, grains, pores, bubbles and inclusions of a second phase. In this case, we may expect the transition from a fine dislocation loop structure to a coarse dislocation forest. In what follows, a coupled model for the calculation of the dislocation density and cavity-size distribution in U-10 wt.% Mo is presented to remedy these shortcomings.

## INTRAGRANULAR SWELLING MODEL

The model consists of a set of coupled equations for the time rate of change of the vacancy ( $c_v$ ) and interstitial ( $c_i$ ) concentrations, the interstitial loop diameter ( $D_l$ ) and density ( $N_l$ ), the density of forest dislocation ( $f_d$ ), the cavity radius ( $r_c$ ) and density ( $c_c$ ), the average number of gas atoms in each cavity ( $N_g$ ), and, the concentration of gas atoms in solution in the fuel ( $c_g$ ). These equations are given by

$$\frac{dc_v}{dt} = K - a_r c_v c_i - k_v b r_l \rho D_l c_v, \quad (1)$$

$$\frac{dc_i}{dt} = K - a_r c_v c_i - k_i b r_l \rho D_l c_i - 16 p D_l c_i c_i / a^2, \quad (2)$$

$$\frac{dN_l}{dt} = 16 p D_l c_i c_i / (\Omega a^2) - p v_l b c_i N_l / D_d, \quad (3)$$

$$\frac{dD_d}{dt} = \frac{2}{a} v_i b_t G, \quad (4)$$

$$\frac{df_d}{dt} = p v_i b_t G N_i - 4 v_i b_t G f_d / d_g, \quad (5)$$

$$\frac{dr_c}{dt} = k_v D_v (c_v - c_v^0) - k_i D_i c_i, \quad (6)$$

$$\frac{dc_g}{dt} = G - 16 p f_n r_g D_g c_g c_g - 4 p r_c D_g c_g c_g + b N_g c_c, \quad (7)$$

$$\frac{dc_c}{dt} = 16 p f_n r_g D_g c_g c_g / N_g - 16 p D_c c_c c_c, \quad (8)$$

$$\frac{dN_g}{dt} = 4 p r_c D_g c_g - b N_g + 16 p N_g r_c D_c c_c, \quad (9)$$

where

$$c_v^0 = c_v^t e^{-\frac{P_g - 2\xi/r_c - \sigma}{\Omega kT}}, \quad (10)$$

$$v_i b_t G = z_i r_i b_t (D_i c_i - z_v r_v b_t (D_v c_v), \quad (11)$$

and

$$r_i b_t G = p N_i D_i. \quad (12)$$

In the above equations,  $K$  is the damage rate in dpa/s;  $a_r$  is the usual recombination coefficient;  $a$  and  $\Omega$  are the lattice constant and atomic volume, respectively;  $D_v$ ,  $D_i$ , and  $D_g$  are the vacancy, interstitial, and gas-atom diffusivity, respectively;  $k_v b_t r_i$  and  $k_i b_t r_i$  are the vacancy and interstitial sink strengths;  $f_n$  is the gas bubble nucleation factor;  $r_g$  is the gas-atom radius;  $G$  is the gas-atom generation rate in atoms/cm<sup>3</sup>/s;  $D_g$  is the gas-atom diffusivity;  $z_v$  and  $z_i$  are the vacancy and interstitial bias factors;  $c_v^t$  is the thermal equilibrium vacancy concentration;  $P_g$  is the internal gas pressure in the cavity;  $\sigma$  is the external stress on the cavity;  $d_g$  is the grain diameter; and,  $\xi$  is the surface energy.

The vacancy and gas-atom diffusivities are given by

$$D_v = 0.0458 e^{-e_{vm}/kT} + f V^{5/3} / 15, \quad (13)$$

and

$$D_g = D_g^T + f V^{5/3} / 15. \quad (14)$$

$\dot{f}$  is the fission rate in fissions/cm<sup>3</sup>/s,  $e_{vm}$  is the vacancy migration energy, and  $D_g^1$  is the thermal component of the gas-atom diffusivity ( $\ll f V^{5/3} / 15$  at ATR temperatures). The irradiation-enhanced diffusion component of  $D_v$  and  $D_g$  was derived on the basis of studies of structural changes taking place in two-phase uranium-molybdenum alloys under the action of neutron irradiation [2]. This assumption is reasonable if the irradiation-induced diffusion mechanism is similar to the irradiation-induced phase mixing mechanism. The volume of thermal spikes important for vacancy diffusion,  $V$ , based on calculations of temperature-time curves in the thermal spike is estimated to be  $8.2 \times 10^{-18}$  cm<sup>3</sup> at 373 K. The irradiation component of  $D_v$  was introduced to achieve physically realistic results at low temperatures for point defect concentrations and a saturated dislocation density. The value of the gas-atom diffusion coefficient given by Eq. 14 lies within the scatter of the measured diffusion coefficients in oxides, mixed oxides, carbides, and nitrides [3].

The dislocation loops evolve according to Eqs. 3 and 4 until the spacing between loops reaches some characteristic distance. It is assumed here that loop nucleation and growth (Eqs.3 and 4, respectively) continue until the loops contact each other, i.e.,

$$D_l \frac{dC_v}{dt} \sqrt{r_l} \frac{dC_l}{dt} = 1 . \quad (15)$$

Eq. 15 yields a similar result as that based on impurity pinning.

## INTRAGRANULAR SWELLING ANALYSIS

Eqs. 1-15 were solved numerically for a fission rate of  $1 \times 10^{14}$  fissions cm<sup>-3</sup> s<sup>-1</sup> and a fuel temperature of 373 K. Figure 1 shows the calculated total dislocation density  $\mathbf{r} = \mathbf{r}_l + \mathbf{f}_d$  as a function of irradiation time for two values of the vacancy migration energy  $e_{vm}$ .  $e_{vm}$  is the critical parameter in the theory for these operating conditions (low temperature and high fission rate). The two values of  $e_{vm}$  used in Fig. 1 correspond to diffusion dominated by radiation processes ( $e_{vm} = 1.1$  eV), and diffusion dominated by thermal processes ( $e_{vm} = 0.75$  eV). The calculations shown in Fig. 1 indicate that the dislocation density reaches a steady-state value for irradiation times greater than  $\approx 6 \times 10^6$  s. This time corresponds to  $\approx 7.5$  at.% burnup of U-10 Mo. A reduction in the value of  $e_{vm}$  from 1.1 to 0.75 eV results in an increase in the calculated dislocation density of more than one order of magnitude (i.e., from  $\approx 10^9$  to  $\approx 10^{10}$  cm<sup>-2</sup>). A decrease in  $e_{vm}$  translates to higher vacancy diffusivities and a higher loss rate of vacancies to sinks such as dislocations and cavities. A decrease in the vacancy concentration causes a reduction in the recombination rate between vacancies and interstitials, and thus an increase in the

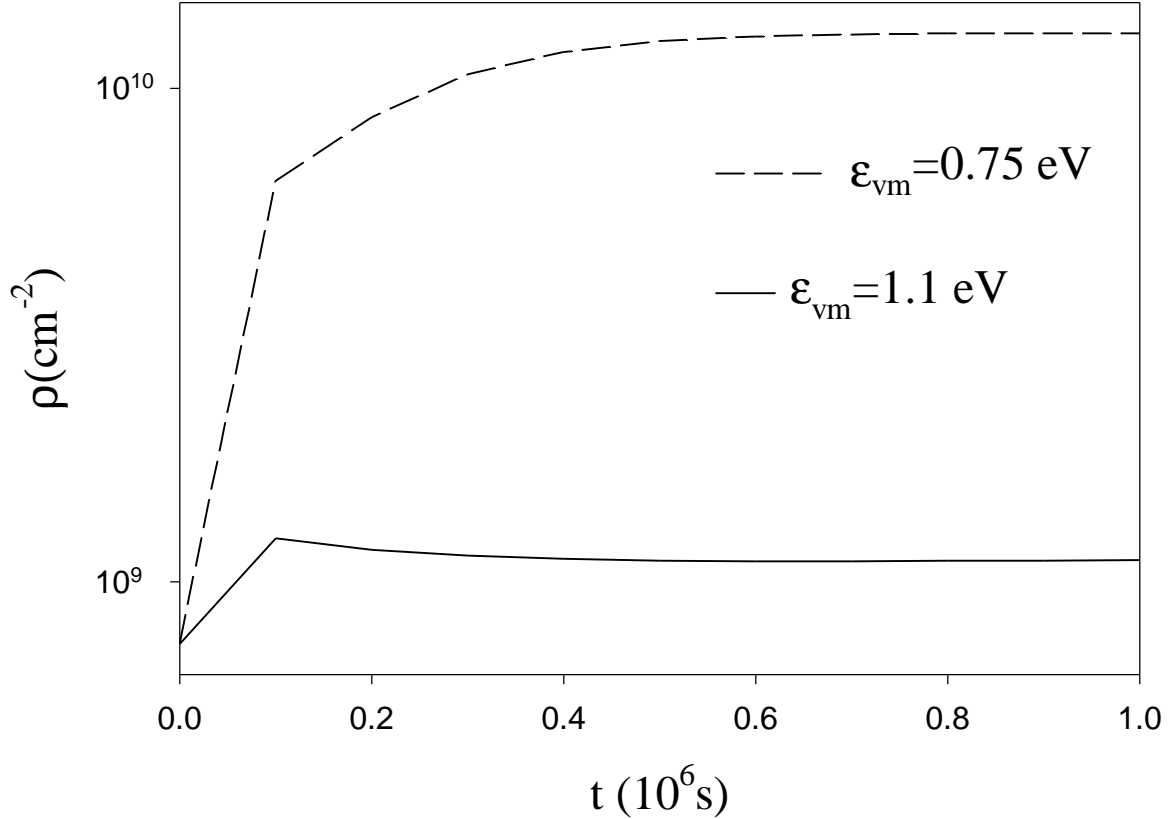


Fig. 1. Calculated total dislocation density  $\mathbf{r} = \mathbf{r}_l + f_d$  as a function of irradiation time for two values of vacancy migration energy  $\mathbf{e}_{vm}$ .

interstitial concentration. A higher interstitial concentration promotes increased loop nucleation and growth and results in a higher value of the dislocation density.

Figure 2 shows the calculated swelling due to intragranular cavities for the same two values of  $\mathbf{e}_{vm}$ . A value for  $\mathbf{e}_{vm}$  of 1.1 eV results in intragranular swelling  $\ll 1\%$  for fuel-particle burnups  $> 40$  at.%. However, a value for  $\mathbf{e}_{vm}$  of 0.75 eV results in cavity-induced intragranular swelling  $> 200\%$ ! The reason for this dramatic more than two-order-of-magnitude increase in swelling for a 25% decrease in vacancy migration energy has its roots in the difference between gas-driven (gas bubble) and bias-driven (void) swelling mechanisms.

In order to understand the nature of cavity swelling in the material, it is instructive to examine the behavior of the excess cavity pressure  $P_g - 2\xi/r_c$  that appears in the exponent in Eq. 10 (in the following, the value of the external pressure  $\mathbf{S}$  is assumed to

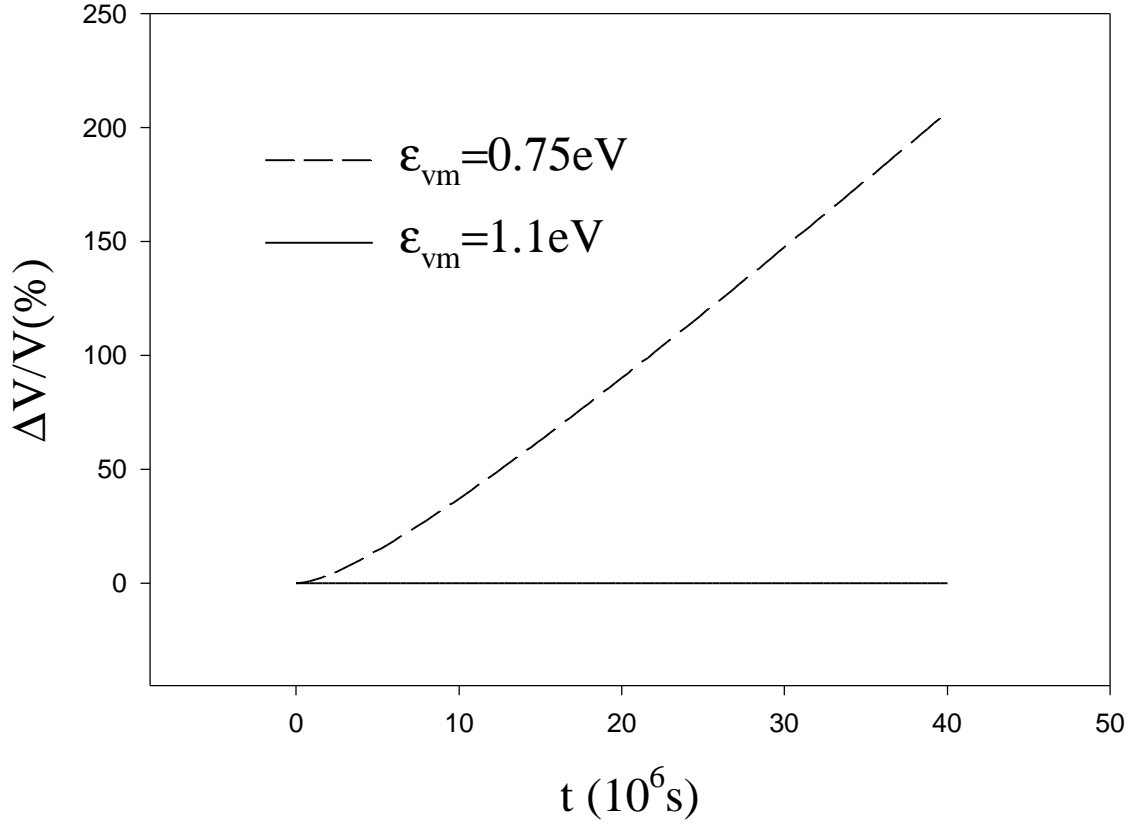


Fig. 2. Calculated swelling due to intragranular cavities for two values of  $\epsilon_{vm}$ .

be negligible). Figure 3 shows the calculated excess cavity pressure for the two values of  $\epsilon_{vm}$  as a function of irradiation time. As shown in Fig. 3, for  $\epsilon_{vm} = 1.1$  eV,  $P_g - 2\epsilon/r_c$  is positive and increasing throughout the irradiation period. This means that the gas pressure within the cavity,  $P_g$ , is greater than the surface tension,  $2\epsilon/r_c$ , and that the cavity is behaving like a gas bubble. The excess cavity pressure increases because of an insufficient number of available vacancies in the matrix required for equilibration. If sufficient vacancies are made available (e.g., by creep processes), bubble growth will continue until the bubbles become equilibrated (excess pressure equal to zero). Continued bubble growth requires the diffusion of gas atoms, as well as vacancies to the bubble. Bubble growth is also limited due to irradiation-induced gas-atom re-solution from bubbles. For these reasons, swelling due to bubble growth is generally well behaved (i.e., linear).

On the other hand, as shown in Fig. 3, for  $\epsilon_{vm} = 0.75$  eV, the excess pressure is negative throughout the entire irradiation period. For this case, the surface tension is

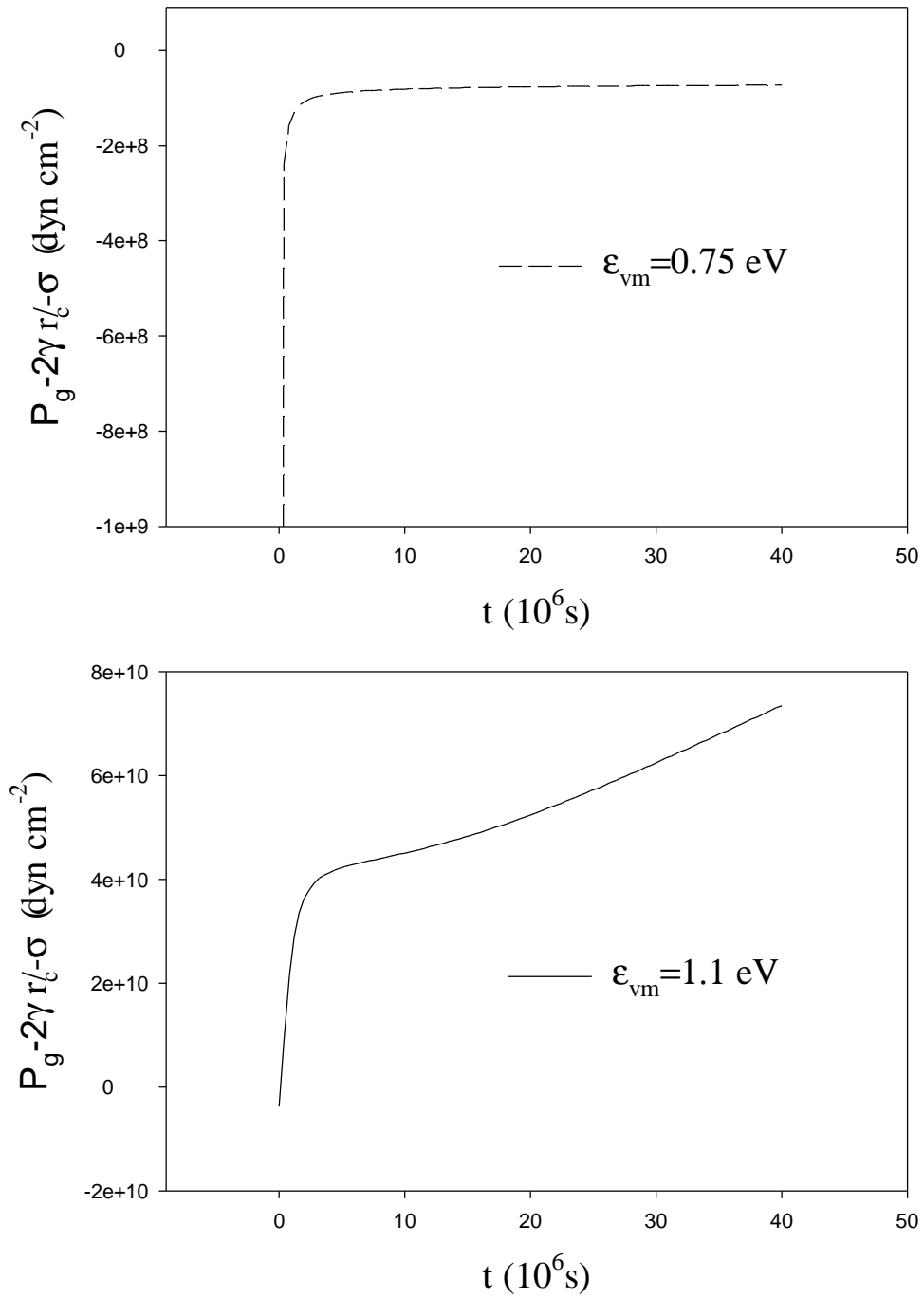


Fig.3. Calculated excess cavity pressure for two values of  $\epsilon_{vm}$  as a function of irradiation time.

greater than the internal gas pressure, and, because the right-hand side of Eq. 6 is positive due to a super-saturation of vacancies in the lattice, the cavity grows by the influx of vacancies. Continued cavity growth under these conditions (bias-driven void growth) requires only excess vacancies in the lattice. For this reason, void growth can lead to unstable swelling behavior.

A key question is whether the irradiation-induced swelling of U-10Mo is bubble- or bias-driven. If bubble driven, the swelling is expected to be stable. If bias-driven, the swelling could become unstable at high burnup, leading to unacceptable materials behavior during irradiation. Given the above analysis, this question can be rephrased as to whether the vacancy migration energy in U-10Mo is closer to 1.1 eV or to 0.75 eV.

It is apparent that the swelling mechanism depends on the ratio of vacancy flux to gas-atom flux into cavities. Subsequent to a steady-state concentration of gas atoms, the flux of gas atoms to cavities equals the gas-atom generation rate. The “accessible” quantity of vacancies is defined by a difference in absorption rate of interstitials and vacancies by dislocations. At low irradiation temperature, where the dominant defect destruction mechanism is recombination, Eqs. 1 and 2 can be simplified and the ratio of vacancy to gas-atom flux into cavities is given by

$$\mathbf{x} = \frac{\sqrt{KD_v D_i}}{K_{xe}} \mathbf{a}_r \mathbf{r}_d (Z_i - Z_v) \quad (16)$$

where  $K_{xe}$  is the production rate of Xe atoms in atom fraction per second. Using the results shown in Fig. 1, we obtain  $\mathbf{x} = 4$  for  $e_{vm} = 1.1$  eV, and  $\mathbf{x} = 25$  for  $e_{vm} = 0.75$  eV.  $\mathbf{x} = 4$  corresponds to a lower limit in the number of vacancies per gas atom in the cavity and represents a liquid-like state in bubbles having sizes of  $\approx 10^{-7}$  cm. This situation is described by the upper graph in Fig. 3, which shows that the small gas bubbles are under intense pressure. An increase in cavity size requires additional vacancies per gas atom, and  $\mathbf{x} \approx 6$  corresponds to a bubble radius of  $\approx 10^{-6}$  cm. At  $\mathbf{x} \approx 25$ , a cavity radius of  $\approx 10^{-5}$  is achieved. These large cavities have an excess of vacancies. This situation corresponds to bias-driven growth and is described by the lower graph in Fig. 3. As shown in Fig. 2, intragranular swelling is extremely sensitive to the cavity growth mechanism.

There is an observed linear relationship between the activation energy of uranium self-diffusion in body-centered cubic metals and the melting point of the metals under consideration [4]. This relationship can be expressed as

$$Q_{self} = kT_{melt} \quad (17)$$

$$k = 1.453 \times 10^{-3} \text{ eV / } \Delta T \text{ at } K.$$

The energy for self-diffusion,  $Q_{self}$ , is related to the vacancy migration,  $e_{vm}$ , and formation,  $e_{vf}$ , energies by

$$Q_{self} = e_{vm} + e_{vf}. \quad (18)$$

In general,  $e_{vm} \approx 0.5Q_{self}$  so that

$$e_{vm} = 7.265 \times 10^{-4} T_{melt} \text{ (eV / K)}. \quad (19)$$

For metastable alloys, such as U-10 wt.% Mo, the assumption is made that the solidus point represents the melting point. For U-10 wt.% Mo, the solidus occurs at 1520 K. Thus, from Eq.18,  $e_{vm} = 1.1$  eV. From the analysis illustrated by Figs. 1-3, and the discussion of Eq. 16 we are forced to the conclusion that any cavities in the lattice of the irradiated U-10 wt.% Mo are gas bubbles and not voids. In addition, the above analysis leads us the opinion that the vacancy migration energy in U-10 Mo is 1.1 eV.

## GRAIN-BOUNDARY SWELLING ANALYSIS

The analysis presented above indicates that intragranular swelling of U-10 Mo is of little concern. Another possible cause of fuel deformation is intergranular swelling. Irradiation-induced recrystallization and enhanced bubble growth on the newly formed grain boundaries was proposed as an interpretation of the observed fission-gas-bubble-size distribution and swelling curve for  $U_3Si_2$  aluminum dispersion fuels and for  $UO_2$  power reactor fuels [5]. Recrystallization and intergranular bubble growth have been definitively confirmed for  $UO_2$  fuels [6]. Based on this experience, it was natural for the authors to suppose that cavities, if observed, should be associated with a subgrain structure.

Figure 4 shows DART-calculated fission-gas-bubble-size distributions for U-10 wt.% Mo irradiated in the ATR to  $\approx 40$  and  $\approx 70$  at.% burnup [7]. The DART irradiation-induced recrystallization model developed for  $U_3Si_2$  and  $UO_2$  fuels was utilized in the calculations. This model predicts that recrystallization occurs at a fuel-particle fission density of  $\approx 2.6 \times 10^{21} \text{ cm}^{-3}$ . The recrystallized grain size is assumed to be 2  $\mu\text{m}$ . Irradiation-induced recrystallization may be assisted (i.e., will occur at a lower burnup) by damage induced in the heavily deformed fuel particles due to grinding during fuel fabrication at  $\approx 500^\circ\text{C}$ . This effect is not included in the calculations shown in Fig. 4. The distribution at  $\approx 40$  at. % burnup exhibits a flattening (decrease in slope) at a bubble diameter between 0.25 and 0.5  $\mu\text{m}$ . This change in slope in the calculated distribution at  $\approx 40$  at. % burnup, and the large-bubble peak (occurring at a bubble diameter of

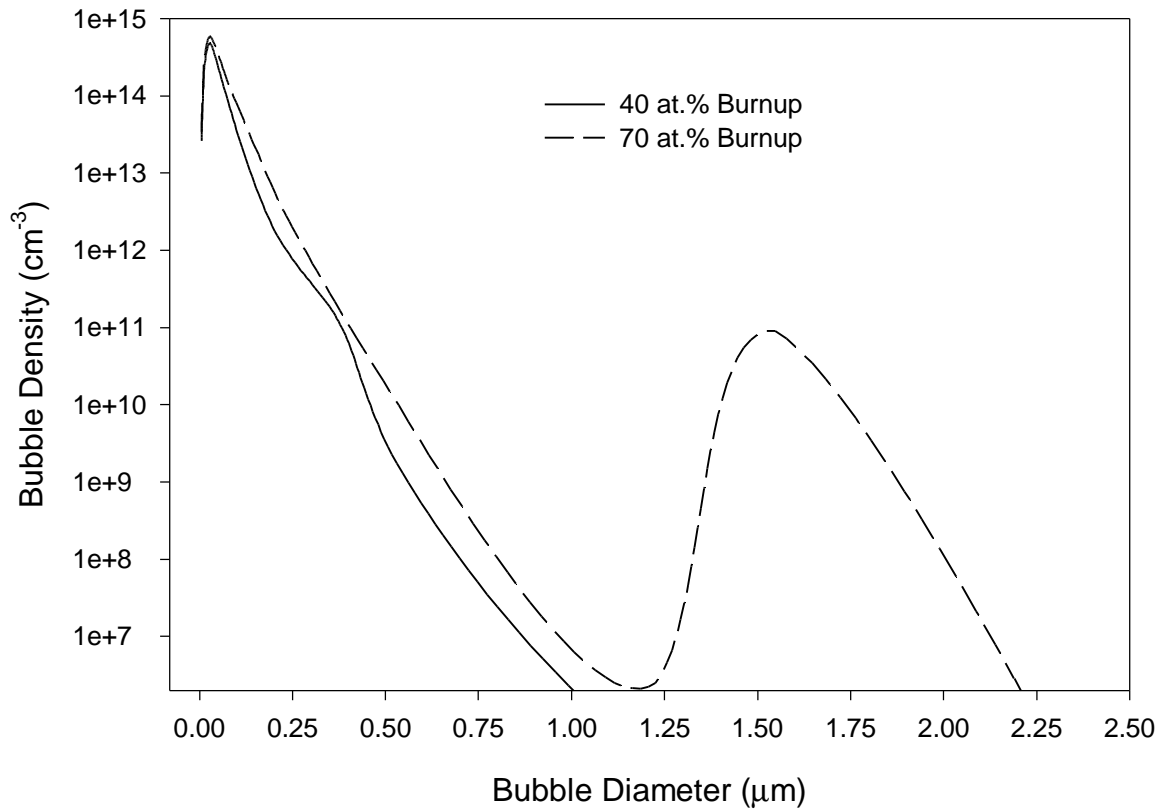
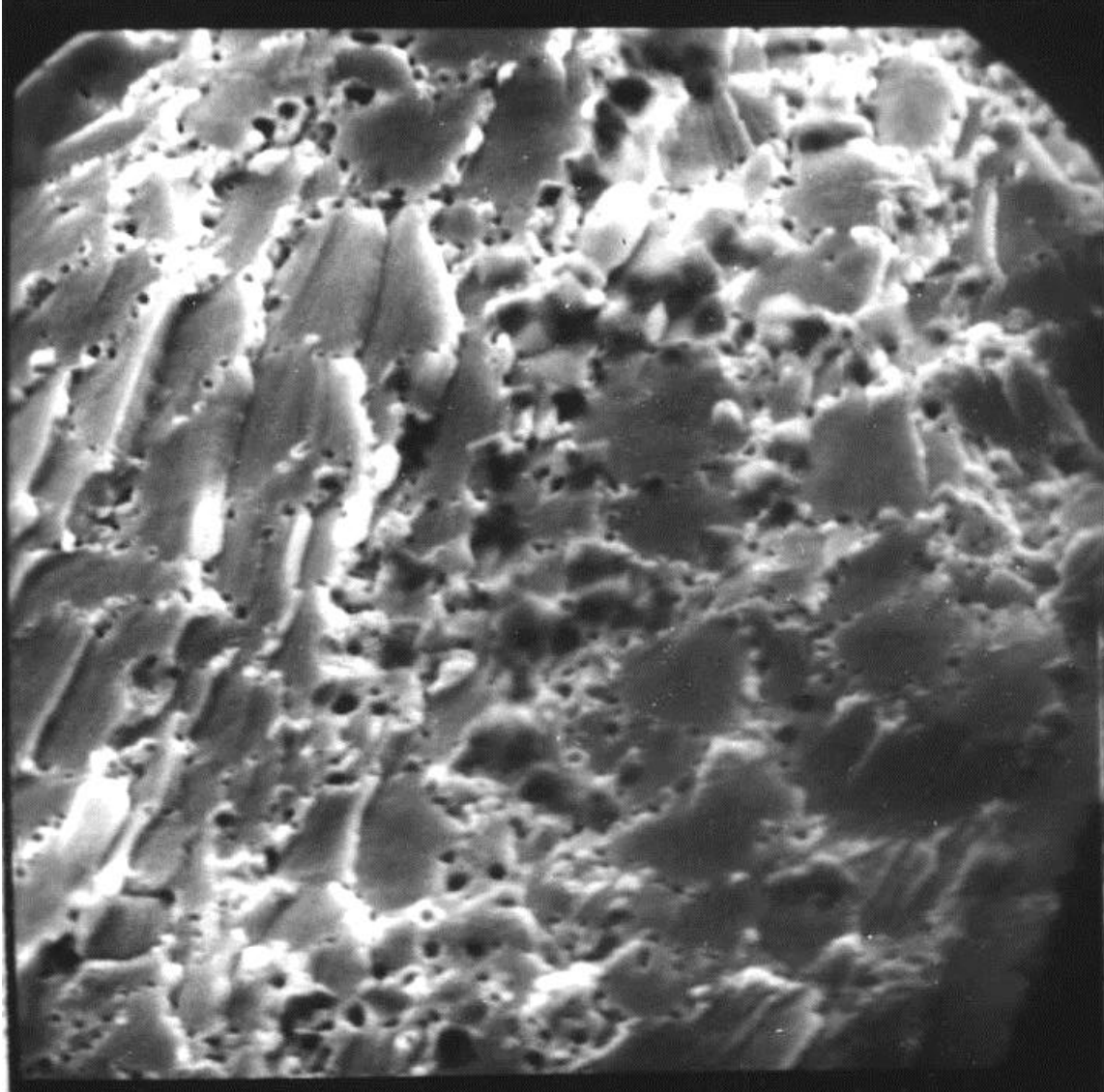


Fig. 4. DART-calculated fission-gas-bubble-size distributions for U-10 wt.% Mo irradiated in ATR to  $\approx 40$  and  $\approx 70$  at.% burnup.

$\approx 1.6 \mu\text{m}$ ) of the bimodal distribution calculated at  $\approx 70$  at. % burnup are associated with grain-corner bubbles. The small-bubble peaks (occurring at a bubble diameter of  $\approx 0.025 \mu\text{m}$ ) in the distributions are associated with grain-boundary bubbles. In the case where fabrication-induced damage leads to an earlier onset of irradiation-induced recrystallization, the larger bubble peak will occur at a larger bubble size. This is because of the longer time that bubbles have to accumulate and grow on the grain boundaries.

The calculated intragranular bubble sizes are well below those resolvable experimentally by scanning electron microscopy (SEM).

Figure 5 shows an SEM micrograph of U-10 wt.% Mo fabricated from ground powder irradiated in the ATR to  $\approx 40$  at.% LEU burnup. Recrystallized grains with diameter  $\approx 2 \mu\text{m}$  and gas bubbles associated with the grain surfaces are clearly seen in



-----  
2.0  $\mu\text{m}$

Fig. 5. SEM photomicrograph of U-10 wt.% Mo fabricated from ground powder irradiated in ATR to  $\approx 40$  at. % LEU burnup.

the micrograph. The distribution of bubbles shown in Fig. 5 contains a distinct population of bubbles having an average size of  $\approx 0.25\text{-}0.5 \mu\text{m}$ . Measured bubble-size distributions are currently not available. However, it is clear that the calculated distributions as shown in Fig. 4 are in qualitative agreement with the observed bubbles shown in Fig. 5.

Figure 6 shows the calculated fuel-particle swelling as a function of particle fission density; 40 at.% burnup occurs at  $\approx 3 \times 10^{27} \text{ m}^{-3}$  and 70 at.% burnup occurs at

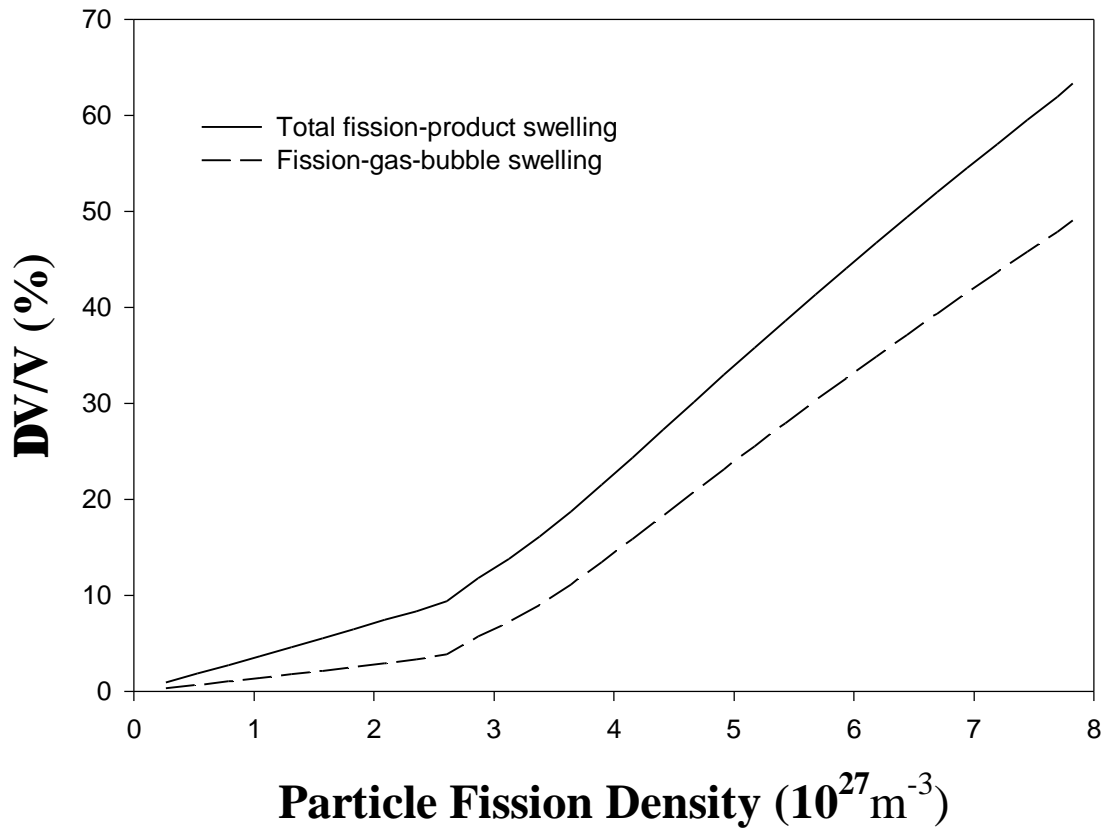


Fig. 6. Calculated fuel-particle swelling as a function of particle fission density.

$\approx 5 \times 10^{27} \text{ m}^{-3}$ . The difference between the fission-gas-bubble swelling (dashed curve) and the total fission-product swelling (solid) curve is the solid-fission product swelling contribution. Swelling due to the interaction between the fuel particle and the aluminum matrix is not included in Fig. 6. As can be seen from the results shown in Fig. 6, the swelling is linear throughout the entire irradiation period. The change in slope of the swelling curves at  $\approx 2.6 \times 10^{27} \text{ m}^{-3}$  is due to irradiation-induced recrystallization. Subsequent to irradiation-induced recrystallization, the swelling rate increases due to enhanced bubble growth on the recrystallized grain surfaces. The total calculated fission-product swelling at 70 at.% burnup is  $\approx 38\%$ : this swelling behavior is similar to that observed for  $\text{U}_3\text{Si}_2$ .

## CONCLUSIONS

SEM photomicrographs of U-10 wt.% Mo irradiated at low temperature in the ATR to  $\approx 40$  at.% burnup show the presence of cavities. We have used a rate-theory-based model to investigate the nucleation and growth of cavities during low-temperature irradiation of uranium-molybdenum alloys in the presence of irradiation-induced interstitial-loop formation and growth. In addition, the evolution of forest dislocations was calculated on the basis of dislocation loop growth and simultaneous climb and glide of unfaulted loops. Consolidation of the dislocation structure takes into account capture of interstitial dislocation loops and loss to grain boundaries. Bias-driven growth of cavities can lead to substantial swelling of the alloy (void swelling). However, our calculations indicate that the swelling mechanism in the U-10 wt.% Mo alloy at low irradiation temperatures is fission-gas-driven. The calculations also indicate that the observed bubbles must be associated with a subgrain structure. Calculated swelling and bubble-size-distribution are in qualitative agreement with the observations. The model predicts that U-10 wt.% Mo will exhibit stable fission-product-swelling behavior throughout its lifetime. Work exploring the effects of alloy composition and temperature on swelling is in progress.

## REFERENCES

1. J. Rest, G. L. Hofman, K. L. Coffey, I. Konovalov, and A. Maslov, "Analysis of the Swelling Behavior of U-Alloys," To be published in proc. 20<sup>th</sup> Int. Meeting on Reduced Enrichment for Research and Test Reactors, Jackson Hole, WY, Oct. 5-11, 1997.
2. S. T. Konobeevsky, K. P. Dubrovin, B. M. Levitsky, L. D. Panteleev, and N. F. Pravdyuk, 2<sup>nd</sup> Geneva Conf. paper 232, 1958.
3. HJ. Matzke, in Diffusion Processes in Nuclear Materials, R.P. Agarwala, editor, Elsevier Science Publishers B.V. (1992) 9-69
4. G. B. Fedorov and E. A. Smirnov, "Diffusion in Reactor Materials," Published for the National Bureau of Standards, U.S. Dept. of Commerce and the National Science Foundation, Washington, DC, by Amerind Publishing Co. Pvt. Ltd., New Delhi, India (1984)
5. J. Rest and G. L. Hofman, J. Nucl. Mater., 210 (1994) 187-202.
6. K. Nogita and K. Une, Nucl. Instr. and Meth. B 91 (1994) 301.
7. J. Rest, "The DART Dispersion Analysis Research Tool: A Mechanistic Model for Predicting Fission-Product-Induced Swelling of Aluminum Dispersion Fuels," Argonne National Laboratory Report ANL-95/36 (Aug. 1995).